Appraisal of state-of-the-art

Improvement of acquisition and analysis methods in multi-electrode array experiments with iPS cell-derived cardiomyocytes

Keiichi Asakura [a,b,c,d,e], Seiji Hayashi [a,b,e], Atsuko Ojima [b,f], Tomohiko Taniguchi [b,c,d,f,*], Norimasa Miyamoto [b,c,d,f], Chiaki Nakamori [d,g], Chiho Nagasawa [d,g], Tetsuo Kitamura [d,h], Tomoharu Osada [a,b,h], Yayoi Honda [d,i], Chieko Kasai [a,b,j], Hiroyuki Ando [a,b,k], Yasunari Kanda [a,b,l], Yuko Sekino [a,b,l], Kohei Sawada [a,b,f]

[a] Japanese Safety Pharmacology Society (JSPS), 3-39-22 Showa-machi, Maebashi, Gunma 371-8511, Japan
[b] Japan iPS Cardiac Safety Assessment (JiCSA), 1-18-1 Kamiyoga, Setagaya-ku, Tokyo 158-8501, Japan
[c] Non-Clinical Evaluation Expert Committee, Drug Evaluation Committee, Japan Pharmaceutical Manufacturers Association (JPMA), 2-3-11 Nihonbashi-Honcho, Chuo-ku, Tokyo 103-0023, Japan
[d] Consortium for Safety Assessment using Human iPS Cells (CSAHi), Japan
[e] Nippon Shinyaku Co., Ltd., 14, Nishinosho-Monguchi-cho, Kisshoin, Minami-ku, Kyoto 601-8550, Japan
[f] Eisai Co., Ltd., 5-1-3 Tokodai, Tsukuba, Ibaraki 300-2635, Japan
[g] Taisho Pharmaceutical Co., Ltd., 1-403 Yoshino-cho, Kita-ku, Saitama, Saitama 331-9530, Japan
[h] LSI Medience Corporation, 13-4 Uchikanda 1-chome, Chiyoda-ku, Tokyo 101-8517, Japan
[i] Sumitomo Dainippon Pharma Co., Ltd., 3-1-98 Kasugade-naka, Konohana-Ku, Osaka 554-0022, Japan
[j] Astellas Pharma Inc., 2-1-6 Kashima, Yodogawa-ku, Osaka 532-8514, Japan
[k] Ono Pharmaceutical Co., Ltd., 50-10 Yamagishi Mikuni-cho, Sakaishi, Fukui 913-8538, Japan
[l] National Institute of Health Sciences (NIHS), 1-18-1 Kamiyoga, Setagaya-ku, Tokyo 158-8501, Japan

ARTICLE INFO

ABSTRACT

Introduction: Multi-electrode array (MEA) systems and human induced pluripotent stem (iPS) cell-derived cardiomyocytes are frequently used to characterize the electrophysiological effects of drug candidates for the prediction of QT prolongation and proarrhythmic potential. However, the optimal experimental conditions for obtaining reliable experimental data, such as high-pass filter (HPF) frequency and cell plating density, remain to be determined.
Methods: Extracellular field potentials (FPs) were recorded from iPS cell-derived cardiomyocyte sheets by using the MED64 and MEA2100 multi-electrode array systems. Effects of HPF frequency (0.1 or 1 Hz) on FP duration (FPD) were assessed in the presence and absence of moxifloxacin, terfenadine, and aspirin. The influence of cell density on FP characteristics recorded through a 0.1-Hz HPF was examined. The relationship between FP and action potential (AP) was elucidated by simultaneous recording of FP and AP using a membrane potential dye.
Results: Many of the FP waveforms recorded through a 1-Hz HPF were markedly deformed and appeared differentiated compared with those recorded through a 0.1-Hz HPF. The concentration–response curves for FPD in the presence of terfenadine reached a steady state at concentrations of 0.1 and 0.3 μM when a 0.1-Hz HPF was used. In contrast, FPD decreased at a concentration of 0.3 μM with a characteristic bell-shaped concentration–response curve when a 1-Hz HPF was used. The amplitude of the first and second peaks in the FP waveform increased with increasing cell plating density. The second peak of the FP waveform roughly coincided with AP signal at 50% re-polarization, and the negative deflection at the second peak of the FP waveform in the presence of E-4031 corresponded to early afterdepolarization and triggered activity.
Discussion: FP can be used to assess the QT prolongation and proarrhythmic potential of drug candidates; however, experimental conditions such as HPF frequency are important for obtaining reliable data.

* Corresponding author at: Biopharmaceutical Assessments Core Function Unit, Eisai Product Creation Systems, Eisai Co., Ltd., 5-1-3 Tokodai, Tsukuba, Ibaraki 300-2635, Japan. Tel.: +81 29 847 5754; fax: +81 29 847 2037.
  E-mail address: t2-taniguchi@hhc.eisai.co.jp (T. Taniguchi).
  URL's: http://www.j-sps.org/, http://jicsa.org/, http://csahi.org/en/ (K. Asakura), http://www.j-sps.org/, http://jicsa.org/, http://csahi.org/en/ (S. Hayashi), http://jicsa.org/ (A. Ojima), http://jicsa.org/, http://csahi.org/en/ (T. Taniguchi), http://jicsa.org/, http://csahi.org/en/ (N. Miyamoto), http://csahi.org/en/ (C. Nakamori), http://csahi.org/en/ (C. Nagasawa), http://csahi.org/en/ (T. Kitamura), http://www.j-sps.org/, http://jicsa.org/ (T. Osada), http://csahi.org/en/ (Y. Honda), http://www.j-sps.org/, http://jicsa.org/ (C. Kasai), http://www.j-sps.org/, http://jicsa.org/, http://csahi.org/en/ (H. Ando), http://www.j-sps.org/, http://jicsa.org/ (Y. Kanda), http://www.j-sps.org/, http://jicsa.org/ (Y. Sekino), http://www.j-sps.org/, http://jicsa.org/ (K. Sawada).

1. Introduction

Drug-induced QT interval prolongation is a major cause of ventricular tachycardia such as torsade de pointes, and the majority of drugs known to induce QT prolongation preferentially target the human ether-a-go-go-related gene (hERG) channel (Redfern et al., 2003). The QT prolongation potential of drug candidates is evaluated by preclinical *in vitro* I_{Kr} (rapid component of delayed rectifier K^+ current) assays and *in vivo* QT experiments and the clinical "thorough QT/QTc study". However, there are often discrepancies between the results obtained through *in vitro* I_{Kr} assays and those obtained through *in vivo* QT experiments, that is, some compounds can give false-negative or false-positive results for QT prolongation *in vivo* (Gintant, 2011; Obiol-Pardo, Gomis-Tena, Sanz, Saiz, & Pastor, 2011). The main reasons for this are that ion channels other than the hERG channel can be involved in drug-induced QT prolongation, and that some compounds, such as multi-channel blockers, do not prolong action potential duration (APD) (Hayashi et al., 2005; Lu et al., 2008; Martin et al., 2004). Therefore, screening models for integrated assessment of multiple cardiac ion channels are expected.

Human cardiomyocytes differentiated from human embryonic stem cells or induced pluripotent stem (iPS) cells, which physiologically express multiple cardiac ion channels, have been increasingly used for the evaluation of drug-induced QT-like-interval prolongation (Gibson, Yue, Bronson, Palmer, & Numann, 2014; Nozaki et al., 2014; Peng, Lacerda, Kirsch, Brown, & Bruening-Wright, 2010; Yamazaki et al., 2012) and the assessment of proarrhythmic potential based on the analysis of early afterdepolarization (EAD) and triggered activity (TA) (Nakamura et al., 2014), short-term variability of repolarization time (Yamazaki et al., 2014), and repolarization delay.

Major technologies for the recording of the electrical activity of cardiomyocytes include intracellular recordings using sharp or patch electrodes, extracellular recordings using multi-electrode arrays (MEAs), and optical imaging using voltage-sensitive dyes (VSDs). Intracellular recording of action potentials (AP) is currently the 'gold standard' method, but it is unsuitable in the early stage of drug development because it requires qualified technicians and is laborious and low-throughput. In contrast, extracellular recording of field potential (FP) by MEA methods or AP measurement using VSD have intermediate throughput and can easily be installed within the current screening flow used for the assessment of proarrhythmic potential.

Since Thomas, Springer, Loeb, Berwald-Netter, and Okun (1972) first reported the recording of FP in cultured chick embryonic cardiomyocytes by means of a planar MEA, the theory, recording apparatus, and analytical methods have been further developed, mainly for analyzing neuronal network activity (Fejtl, Stett, Nisch, Boven, & Möller, 2006), and these systems are now widely used for the detection of neuronal spikes (Pine, 2006; Spira & Hai, 2013). This technology has also been used to analyze the propagation of APs in cultured cardiomyocyte sheets or clusters from chick, mouse, or rat by detecting sharp spike signals derived from the fast influx of sodium ions (I_{Na}) during the upstroke phase of the AP (Meiry et al., 2001; Egert & Meyer, 2005; Egert et al., 2006). In these studies, high-pass filters (HPF) at around 1 Hz were used to eliminate the drift of baseline caused by very low-frequency electrical signal oscillation. HPFs are implemented by using a resistance–capacitor circuit, which also acts as a differentiator, and a HPF with a frequency of 1 Hz will not affect the detection of neural spikes or the fast depolarization phase of the AP, because the activation kinetics is within the range of several milliseconds.

FP duration (FPD) is defined as the time interval between the start of the first sharp deflection in the waveform (Na^+-channel activation during membrane depolarization) to the peak of the second positive deflection (K^+-channel activation during membrane repolarization) and is considered an index of APD (Meyer, Boven, Günther, & Fejtl, 2004). FPD has been used to evaluate repolarization time in human cardiomyocytes derived from embryonic stem cells or iPS cells (Harris et al., 2013; Kaneko et al., 2014; Tanaka et al., 2009). In these studies, a HPF with a frequency of 1 Hz was used in the detection of the FP and analyses of the FPD. Because the APs of human cardiomyocytes have a long plateau phase, FP signals likely contain low-frequency components around 1 Hz in the plateau and repolarization phases, and consequently waveforms obtained by using a 1-Hz HPF may be altered compared with the raw waveform.

Because the utilization of human cardiomyocytes for the assessment of QT prolongation and proarrhythmic potential is becoming important, as indicated by the Comprehensive *in vitro* Proarrhythmia Assay (CiPA) proposal to evaluate proarrhythmic risk based on mechanistic electrophysiologic understanding of proarrhythmia (Cavero, 2014; Cavero & Holzgrefe, 2014, Sager, Gintant, Turner, Pettit, & Stockbridge, 2014), a higher quality of experimental data and interpretation are now needed. MEA-based assays are already being used in drug screening; however, there are limited reports on the theory and optimal experimental conditions for using this technology for the assessment of the AP repolarization phase in cardiomyocyte sheets.

Here, the Japanese Safety Pharmacology Society (JSPS), Consortium for Safety Assessment using Human iPS Cells (CSAHi), and Japan iPS Cardiac Safety Assessment (JiCSA) have jointly conducted a series of MEA-based experiments using iPS cell-derived cardiomyocytes to examine the effects of HPF filtering and cell plating density on the assessment of proarrhythmic potential. Two MEA systems, MED64 (Alpha MED Scientific) and MEA2100 (MC_Rack, Multi Channel Systems), were used. In addition, the relationship between FP and AP was examined by simultaneously recording FPs and APs by using a VSD.

2. Methods

2.1. Cell culture and plating

Cryopreserved human iPS cell-derived cardiomyocytes (iCells Cardiomyocytes; Cellular Dynamics International, Madison, WI, USA) were obtained and prepared according to the manufacturer's protocol. Briefly, the cells were immediately thawed in iCell Cardiomyocytes Plating Medium (Cellular Dynamics International) and then plated (approximately 2.5×10^6 cells/well) on 6-well tissue-culture plates (Becton Dickinson, Franklin Lakes, NJ, USA; Asahi Glass Inc., Tokyo, Japan; Sumitomo Bakelite Co., Ltd., Tokyo, Japan), which were coated with 0.1% gelatin. Two days after plating, the plating medium was replaced with iCell Cardiomyocytes Maintenance Medium (Cellular Dynamics International). The maintenance medium was used as the culture medium throughout the experiments and was replaced every 2 days. The cells were cultured for 5 to 7 days at 37 °C under an atmosphere of 5% CO_2 and then re-plated onto multi-electrode probes.

The recording areas of multi-electrode probes (MED64 probe: MED-P515A; Alpha Med Scientific, Osaka, Japan; MEA2100 probes: 60MEA200/30iR-Ti-gr and 6-well MEA200/30iR-Ti-tcr; Multi Channel Systems, Reutlingen, Germany) were coated with 2 μL of fibronectin (50 mg of fibronectin in 1 mL of distilled water or Dulbecco's phosphate-buffered saline [−]) and incubated at 37 °C for at least 1 h. The cells cultured in the 6-well tissue-culture plates were dispersed with 0.25% trypsin–EDTA or TrypLE Select (Invitrogen, Carlsbad, CA, USA), re-plated onto the multi-electrode probes at a density of 1.5 to 3.0×10^4 cells in 2 μL of culture medium, and incubated for 1 to 3 h at 37 °C under an atmosphere of 5% CO_2. Each well was then filled with culture medium at a volume of 0.25 mL/well for 6-well MEA2100 probe, 1 mL/well for single-well MEA2100 probe, and 2 mL/well for single-well MED64 probe, which was replaced every 2 to 3 days thereafter, and the cells cultured for a further 6 to 17 days to obtain a sheet of cardiomyocytes with spontaneous and synchronous electrical automaticity.

2.2. Drugs and chemicals

E-4031 was obtained from Wako Pure Chemical Industries (Osaka, Japan) or synthesized at Eisai Co., Ltd. (Tsukuba, Japan). Aspirin was purchased from Wako Pure Chemical Industries, terfenadine from Sigma-Aldrich (St. Louis, MO, USA), and moxifloxacin from Fluka (Tokyo, Japan). Gelatin was obtained from Sigma-Aldrich. Fibronectin was obtained from Becton Dickinson and Invitrogen.

2.3. Recording of FPs

Prior to recording FPs, the cardiomyocyte sheets were equilibrated for at least 30 min in a CO_2 incubator in fresh culture medium. After equilibration, the probes were transferred to FP measurement apparatus and covered with a lid through which a gas containing 5% CO_2 was provided and kept at 36.5 to 38.0 °C. Analogue FP signals from the spontaneously beating cardiomyocyte sheets were acquired through a 0.1-Hz HPF and a 3.5- to 10-kHz low-pass filter and digitized at 20 kHz by using a MED64 (Alpha Med Scientific) or MEA2100 multi-electrode array system (MC_Rack, Multi Channel Systems). To compare FP waveforms recorded through 0.1-Hz and 1-Hz HPFs, waveforms were first recorded through a 0.1-Hz HPF for 1 min, and then the frequency of the HPF was changed to 1-Hz and the waveforms were again recorded from the same preparation. To examine the effects of the 1-Hz HPF on the drug concentration–response curve for FPD, the experiments were conducted using a 0.1-Hz HPF, after which the waveforms were passed through a 1-Hz HPF off-line and used as data obtained through a 1-Hz HPF. The stability and constancy of the waveforms, inter-spike interval, and FPD were confirmed for at least 20 min before adding vehicle or compound solutions. Compound stock solutions were made in dimethyl sulfoxide at 1000-fold the target concentration and were cumulatively added to the wells at one-thousandth volume. The final concentration of dimethyl sulfoxide was 0.5%. At each concentration, FP waveforms were recorded for at least 10 min and the last 30 beats were used as the dataset for the analyses. Compounds tested were E-4031 (1, 3, 10, and 30 nM), terfenadine (0.01, 0.03, 0.1, and 0.3 μM), moxifloxacin (10, 30, 100, and 300 μM), and aspirin (3, 10, 30, and 100 μM). For strong biphasic electrical pulse stimulation of the cardiomyocytes, a single square wave (0.6 msec; 30–40 μA) was delivered from two bipolar electrodes of 64 electrodes probes in the MED64 system.

2.4. FP data analysis

Baseline FP waveforms with a sharp first positive or negative deflection and a second positive deflection that met the following criteria were used for analysis: first positive or negative peak amplitude ≥ ± 200 μV, second peak amplitude ≥ 15 μV, inter-spike interval < 1715 msec, and FPDcF ≥ 340 msec. After recording the FP waveforms, the amplitude of the initial sharp positive and negative deflection (first peak; μV), amplitude of the secondary slower positive deflection (second peak; μV), FPD (msec), and inter-spike interval (msec) were measured and the data analyzed by using the Mobius QT (ver. 0.5.0, Alpha MED Scientific) and LabChart (ver. 7.3.7 AD Instruments, Colorado, CO, USA) software. FPD was defined as the interval between the start of the first sharp deflection in the waveform to the peak of the second positive deflection. FPD was corrected for beating rate with Fridericia's formula ($FPDcF = FPD / [$inter-spike interval $/ 1000]^{1/3}$). The inter-spike interval and FPDcF of the last 30 waveforms at each experimental concentration were averaged. In the FP signals, EAD was defined as relatively slow negative spikes appearing during the second positive deflection (repolarization phase), and TA was defined as one or more FP signals following EAD with a sharp positive or negative deflection and an amplitude ≥ ± 100 μV. When EAD or TA was observed, the data at this concentration were excluded from the statistical analysis.

2.5. Imaging of VSD signals

Cardiomyocytes plated on MED64 probes were stained by using a FluoVolt Membrane Potential Kit (Life Technologies, Carlsbad, CA, USA). Briefly, voltage-sensitive FluoVolt dye was diluted 1:10 with PowerLoad concentrate and mixed with a vortex mixer. The mixture was then further diluted 1:10 with Dulbecco's phosphate-buffered saline (−) and used as 1000× loading dye. The loading dye was added to the culture medium and the cells were incubated for 15 to 20 min at 37 °C under an atmosphere of 5% CO_2 on the stage of an inverted fluorescence microscope (IX71, Olympus, Tokyo, Japan). Confocal images were acquired through a 30× silicone oil immersion objective (numeric aperture, 1.05; working distance, 0.8 mm). Membrane staining was visualized with a Sapphire 488 HP Laser System (Coherent, Inc., Santa Clara, CA, USA) by using standard fluorescein isothiocyanate filter settings (excitation, none; emission, 520/35). Images were recorded with an exposure time of 10.35 msec at 94 frames per second with a confocal scanner (CSU-W1, Yokogawa Electric Cooperation, Tokyo, Japan) and an EMCCD camera with 512 × 512 active pixels (DU897, Andor Technology Ltd., Belfast, UK), and then analyzed by using the Andor iQ (ver. 2.9.1, Andor) and Csu-Pro (ver. 3.0, LUCIR Inc., Ibaraki, Japan) software. All of the microscopy equipment and most of the scanner were enclosed within a transparent cover (Tokken, Inc., Chiba, Japan) to prevent fluctuations in internal temperature, humidity, and CO_2 concentration.

2.6. Statistical analysis

Data are presented as mean ± SEM. The effects of E-4031 on APD and FPD were analyzed with the Prism 6.02 software (GraphPad, La Jolla, CA, USA). Statistical analysis was performed by using paired t-test. $P < 0.05$ was considered statistically significant.

3. Results

3.1. Background of MEA-based recording of FP and AP-like signals

A multi-electrode array can be used to detect changes in the extracellular voltage of a cardiomyocyte sheet, because the slow diffusion of ions between the cleft and bulk solutions means that the electrode array will detect only changes in current (I_{seal}) flowing through R_{seal} within the cleft as described in Fig. 1A. Because cardiomyocytes are smaller in size than the electrode (see Fig. 5A) and because they are tightly connected via gap junctions, each electrode in the array detects the changes in voltage of several cardiomyocytes. The degree of contact between the cardiomyocyte sheet and the electrode greatly affects the accuracy of the FP waveforms recorded (Fig. 1B). When the resistance of the seal formed between the cell sheet and the electrode is high enough for the electrical circuit between the cell sheet and electrodes to be regarded as a simple resistance–capacitor circuit, it is theoretically possible to record waveforms that are similar to those produced by recording AP intracellularly. In the present study, we were able to convert FP signals into AP-like signals during basal measurement by applying a strong electrical pulse to the electrode to make the plasma membrane slightly leaky (Fig. 1C). These AP-like signals were recorded only when a 0.1-Hz HPF was used.

3.2. Effect of HPF frequency on FP waveform

FP waveforms were recorded from the same cardiomyocyte preparation through a 0.1- or 1-Hz HPF (Fig. 2). Typical FP waveforms and AP-like waveforms were observed when a 0.1-Hz HPF was used (Fig. 2A); however, only FP waveforms were observed when a 1-Hz HPF was used (Fig. 2B). Although the waveforms recorded by some of the electrodes were similar irrespective of the HPF used (Fig. 2C, electrode No. 4), the waveforms recorded by others markedly differed depending on the HPF used (Fig. 2C, electrodes No. 5 and No. 47). For
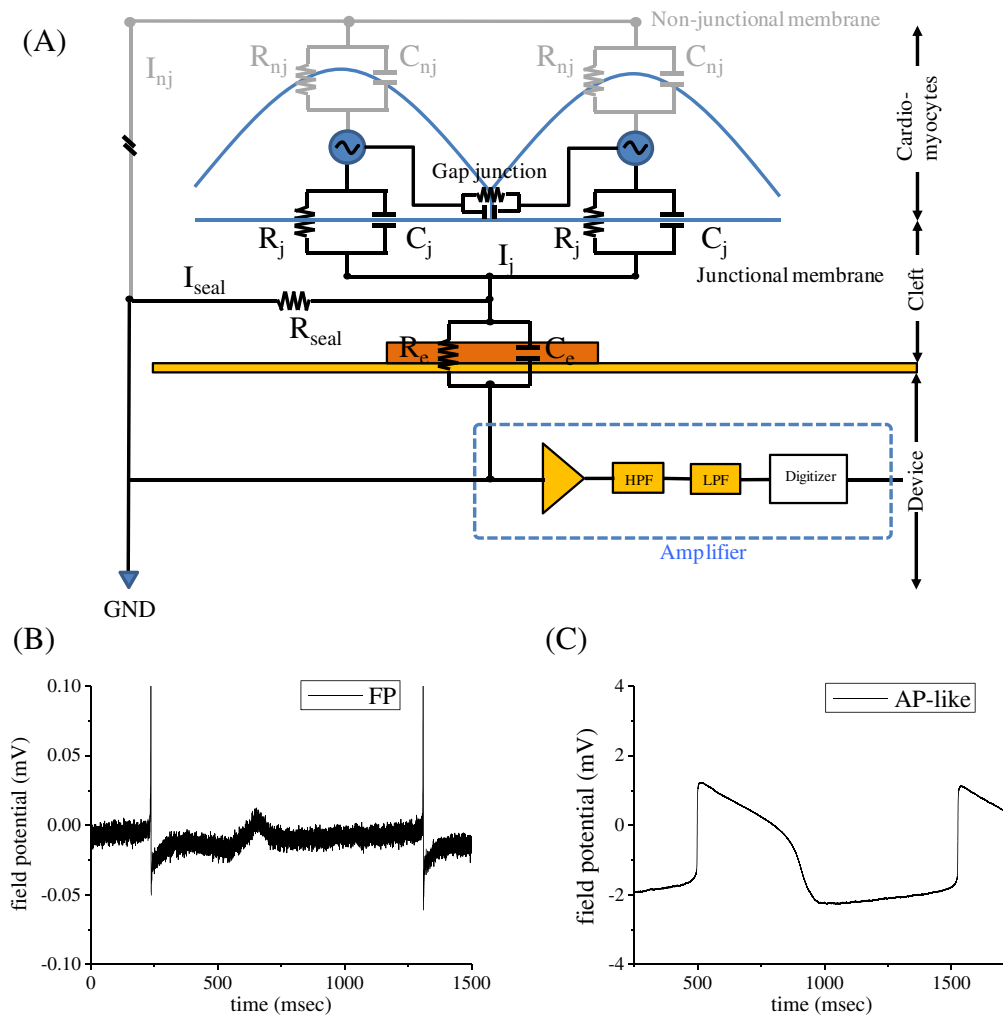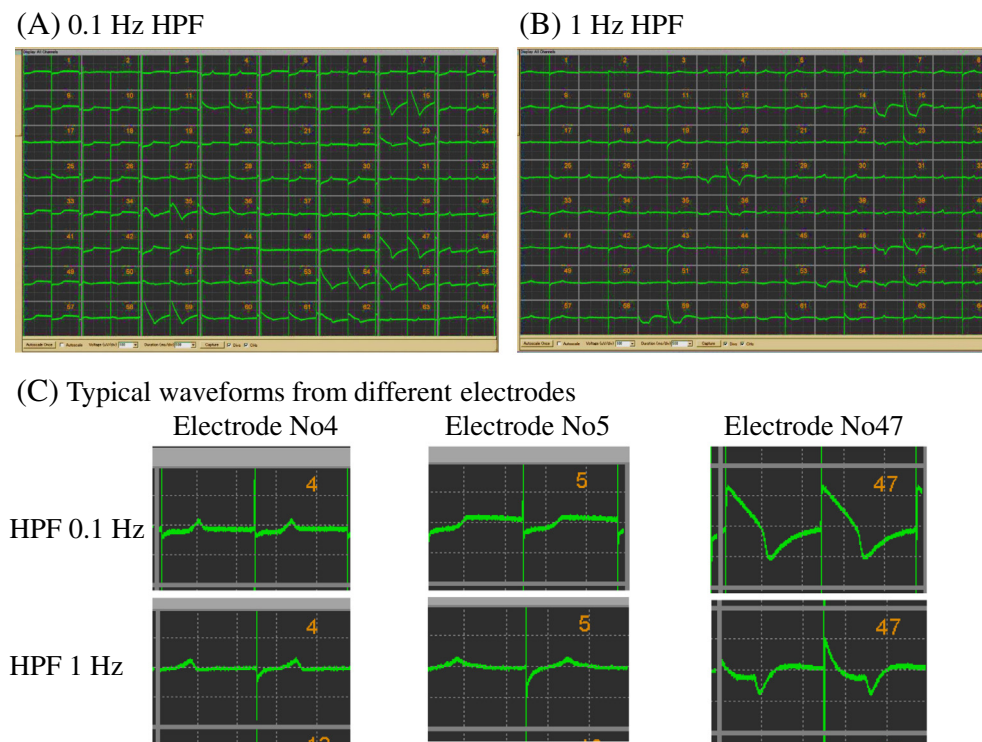
Fig. 1. Schematic layout showing the spatial relationship between the cardiomyocyte cell sheet, a substrate-integrated electrode, and the passive analogue electrical circuit. (A) The cardiomyocyte sheet (blue) resides on a sensing electrode (orange) integrated in the culture substrate (yellow). The electrode is coupled to an amplifier. A cleft filled with culture medium (ionic solution) interposes between the cell membrane and the electrode–substrate. The cardiomyocyte plasma membrane can be divided into two parts: the part that faces the electrode is defined as the junctional membrane and is represented by the junctional membrane resistance (R_j) and the junctional membrane capacitance (C_j). The rest of the membrane, which is defined as the non-junctional membrane, faces the bathing solution and the culture substrate. This part of the membrane is represented by the non-junctional resistance (R_{nj}) and the non-junctional capacitance (C_{nj}) (gray). The physiological solution within the cleft generates the seal resistance (R_{seal}) to ground (GND). Electrode impedance is represented by the electrode resistance (R_e) and electrode capacitance (C_e). The electrode can be a passive element or a transistor. The action potential (AP) is conducted into the analogue cell-circuit in-between R_{nj} and R_j. (B) Under physiological conditions, AP is generated by transient changes in the membrane conductance and the electrode detects the field potential (FP). (C) AP-like waveforms were recorded by biphasic electrical stimulation from the same electrode shown in (B), which had extracellular FP signals. Note that, overall, the amplitude of AP-like waveforms reduced over time and the duration of the occurrence of the AP-like waveforms depended on the individual cardiomyocyte sheet, despite the same conditions being used for electrical stimulation.

example, in the waveform recorded by electrode No. 5, the second peak was absent when a 0.1-Hz HPF was used, but present when a 1-Hz HPF was used, indicating that the FPD differed depending on the frequency of the HPF. Similarly, although the waveform recorded by electrode No. 47 was AP-like when a 0.1-Hz HPF was used, it was markedly deformed with a large negative deflection in the second peak when a 1-Hz HPF was used.

3.3. Effect of HPF frequency on FP waveforms recorded in the presence of a drug

The effects of aspirin, terfenadine, moxifloxacin, and dimethyl sulfoxide on FPDcF were examined to investigate whether HPF frequency affected the concentration–response curve (Fig. 3A–D). Application of aspirin and dimethyl sulfoxide had no remarkable effect on any of the parameters recorded through a 0.1-Hz or 1-Hz HPF (Table 1). Moxifloxacin prolonged FPDcF and slightly decreased the beating rate and first and second peak amplitude in a concentration-dependent

manner irrespective of the HPF used. The average rate of FPDcF prolongation (vs. basal control) when recorded through a 0.1-Hz or 1-Hz HPF was 5.9% and 5.9%, respectively, at 10 μM, 15.8% and 14.0% at 30 μM, and 42.7% and 35.7% at 100 μM. Terfenadine prolonged FPDcF, and the average rate of FPDcF prolongation (vs. basal control) when recorded through a 0.1-Hz or 1-Hz HPF was 5.9% and 6.9%, respectively, at 0.01 μM, 11.9% and 13.6% at 0.03 μM, 18.2% and 14.2% at 0.1 μM, and 16.4% and 4.0% at 0.3 μM. The concentration–response curve for first peak amplitude in the presence of terfenadine was decreased in a dose-dependent manner, and that for second peak amplitude was bell-shaped. The changes in the concentration–response curves, except for those in the concentration–response curve for FPDcF in the presence of terfenadine, were similar irrespective of the HPF used. Comparable results were obtained when FPD was corrected using Bazett's formula (data not shown). In addition, compared with when a 1-Hz HPF was used, the second peak in the FP waveform when a 0.1-Hz HPF was used became increasingly flattened with increasing terfenadine concentration (Fig. 3E).

(A) 0.1 Hz HPF   (B) 1 Hz HPF

(C) Typical waveforms from different electrodes

Electrode No4   Electrode No5   Electrode No47

HPF 0.1 Hz

HPF 1 Hz

Fig. 2. Field potential waveforms of iPS cell-derived cardiomyocytes plated at a density of 30,000 cells/2 μL were recorded with a MED64 multi-electrode array system (Alpha Med Scientific, Osaka, Japan) through a 0.1-Hz (A) or 1-Hz (B) high-pass filter (HFP). After recording the waveforms through a 0.1-Hz HPF for 1 min (A), the frequency of the HPF was changed to 1 Hz and the waveforms were again recorded from the same preparation (B). (C) Typical waveforms of different shapes observed in (A) and (B).

3.4. Effect of cell density on FP parameters and response to E-4031

The effect of cardiomyocyte plating density (15,000, 20,000, or 25,000 cells/2 μL/well) on several FP parameters was examined. The number of electrodes that fulfilled the criteria of first peak amplitude $\geq \pm 200$ μV and second peak amplitude ≥ 15 μV was increased with increasing cell density (Fig. 4A). The average amplitude of both the first and second peaks also increased as cell density increased. Beating rate significantly decreased at a plating density of 15,000 cells, whereas FPDcF was comparable at all three plating densities examined. The concentration–response curves for beats per minute and FPDcF, and the incidence of EAD or TA, in the presence of E-4031 (I_{Kr}-specific blocker) were analyzed by using waveforms that fulfilled the above criteria under basal conditions and had a shape similar to that shown in Fig. 2C (electrode No 4.) No differences in the concentration–response curves or the incidence of EAD or TA were seen at any of the cell plating densities or concentrations of E-4031 examined (Fig. 4B, C, and D). Furthermore, the application of E-4031 had no effect on first peak amplitude (control, 3281.9 ± 193.6 μV vs. 10 nM of E-4031, 3239.1 ± 163.4 μV).

## 3.5. Relationship between FP and AP as assessed by using a VSD

To investigate the relationship between FP and AP in the presence of E-4031, we simultaneously recorded the FP and AP of cardiomyocytes plated on an MED probe by using a VSD optical imaging system and the MED64 multi-electrode array system. VSD imaging showed that the cardiomyocytes were heterogeneous in size and much smaller than the electrodes in the array (Fig. 5A). Because the fluorescence intensity of the cell membrane was stronger than that of the intracellular domain, the tight association of the cardiomyocytes was confirmed. Although FPD is defined as the time between the start of the first sharp deflection and the peak of the second positive deflection in the FP waveform, the relationship between the second peak in the FP waveform and the repolarization phase of the AP is yet to be fully characterized. Therefore, we simultaneously measured APD at 20%, 50%, and 90% repolarization (c, APD_{50}, and APD_{90}), and FPD before and after the addition of 20 nM of E-4031 (the concentration at which APD and FPD were prolonged and EADs were evoked) (Fig. 5B). FPD under basal conditions was comparable to APD_{50}. The presence of E-4031 significantly prolonged both APD_{90} ($P < 0.05$) and FPD ($P < 0.001$), but not APD_{20} and APD_{50}. Next, waveforms were recorded under spontaneous activity and after the addition of 20 or 60 nM of E-4031 (Fig. 5D–E). In the early period after the application of 20 nM of E-4031 (Fig. 5D, left), a single EAD was induced in the AP and a small negative deflection in the second peak was observed in the FP waveform. As exposure time increased (Fig. 5D, right), TA began to appear after the EAD. The addition of 60 nM of E-4031 evoked multiple TA after the EAD in the AP waveform, which corresponded to multiple, sharp negative deflections in the FP waveform.

4. Discussion

4.1. Brief summary

Here we explored the effects of several experimental conditions, including HPF frequency and cell density, to examine whether an MEA system can be used to record high-quality FP data from iPS-derived cardiomyocyte sheets. The relationship between FP and AP was also examined by means of simultaneous measurement of FP and AP. The major findings of this study were as follows: 1) use of a 0.1-Hz HPF caused minimal distortion of the FP waveforms, whereas the use of a 1-Hz HPF in some instances caused marked distortion. Because this distortion may cause misinterpretation of which compounds inhibit hERG channels and induce the depression of the second peak in the FP waveform, HPF frequency was critical for recording accurate FP
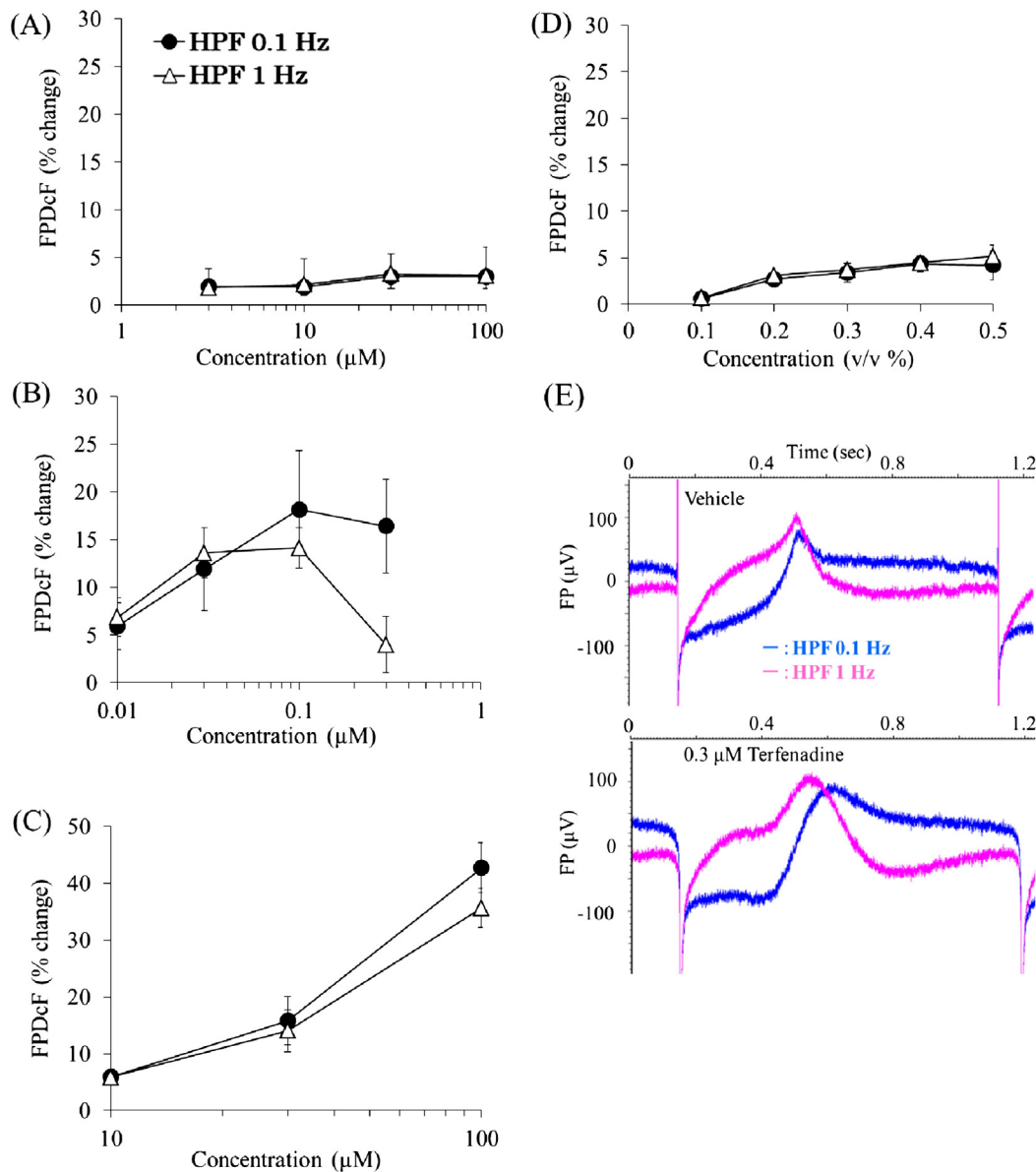
Fig. 3. Comparison of the effect of drug response on field potential duration (FPD) corrected with Fridericia's formula (FPDcF) recorded through a 0.1-Hz or 1-Hz high-pass filter (HPF). Concentration–response curves for (A) aspirin (n = 7), (B) terfenadine (n = 4), (C) moxifloxacin (n = 6 for vehicle and at 10 μM, n = 5 at 30 μM, n = 4 at 100 μM; the size of the dataset was decreased at higher concentrations due to the occurrence of early afterdepolarization), and (D) dimethyl sulfoxide (n = 4). Cells were plated at a density of 15,000 cells/2 μL/well on one of the single-well or 6-well MEA2100 probes and the field potential (FP) waveforms were recorded through a 0.1-Hz HPF for 10 min after application of vehicle (control, 0.1% dimethyl sulfoxide) and then during the cumulative addition of each drug to the required concentrations. A waveform that was similar in shape to that shown in Fig. 2C electrode No. 4 was used for analysis. The waveforms recorded through a 0.1-Hz HPF were passed through a 1-Hz HPF off-line and used as the data obtained through a 1-Hz HPF. Average FPDcF was calculated from the last 30 FPDs during the 10-min recording at each concentration. Data are presented as mean ± SEM for HPF 0.1-Hz (●) and 1-Hz (△). (E) Typical FP waveforms obtained through a 0.1-Hz and a 1-Hz HPF. Representative FP waveforms obtained through a 0.1-Hz HPF were passed through a 1-Hz HPF off-line without the presence of drug (upper panel) and with 0.3 μM terfenadine (lower panel). Note that the second peak of FP waveform in the presence of terfenadine was shifted to the left at 1-Hz HPF was used.

waveforms. 2) A higher density of cells on the MEA electrode produced FP waveforms with higher peak amplitudes and a higher number of electrodes that passed our criteria for inclusion in the analysis of compound effects. 3) FPD at basal conditions corresponded to APD$_{50}$, as assessed by means of a VSD assay, and therefore FPD could be used as a reliable marker of APD. The amplitude and shape of the small negative deflection in the second peak appearing in the FP waveform after drug treatment may be used to discriminate between EAD and TA. 4) When a 0.1-Hz HPF was used, it was possible to record AP-like waveforms without any additional treatment or the application of strong electrical pulses; therefore, these AP-like waveforms may potentially be used to support the interpretation of changes in FP. In conclusion, it is likely that MEA-based experiments using iPS-derived cardiomyocytes to

evaluate QT prolongation and proarrhythmic potentials would be much improved if these findings were taken into account.

4.2. Effect of HPF frequency on FP waveform

A phase shift in the input signal pulse may occur as it passes through the differentiation circuit; therefore, extracellular FP signals recorded with an MEA system through a HPF will show characteristics of differentiation. Commercially available MEA systems such as the MED64 and MEA2100 systems used in the present study use a resistance–capacitor circuit as the HPF in their amplifier (MED64 [Butterworth filter] vs. MEA2100 [Bessel filter]). In the present study, the shape of the second peak was influenced by the HPF when the frequency of the HPF was
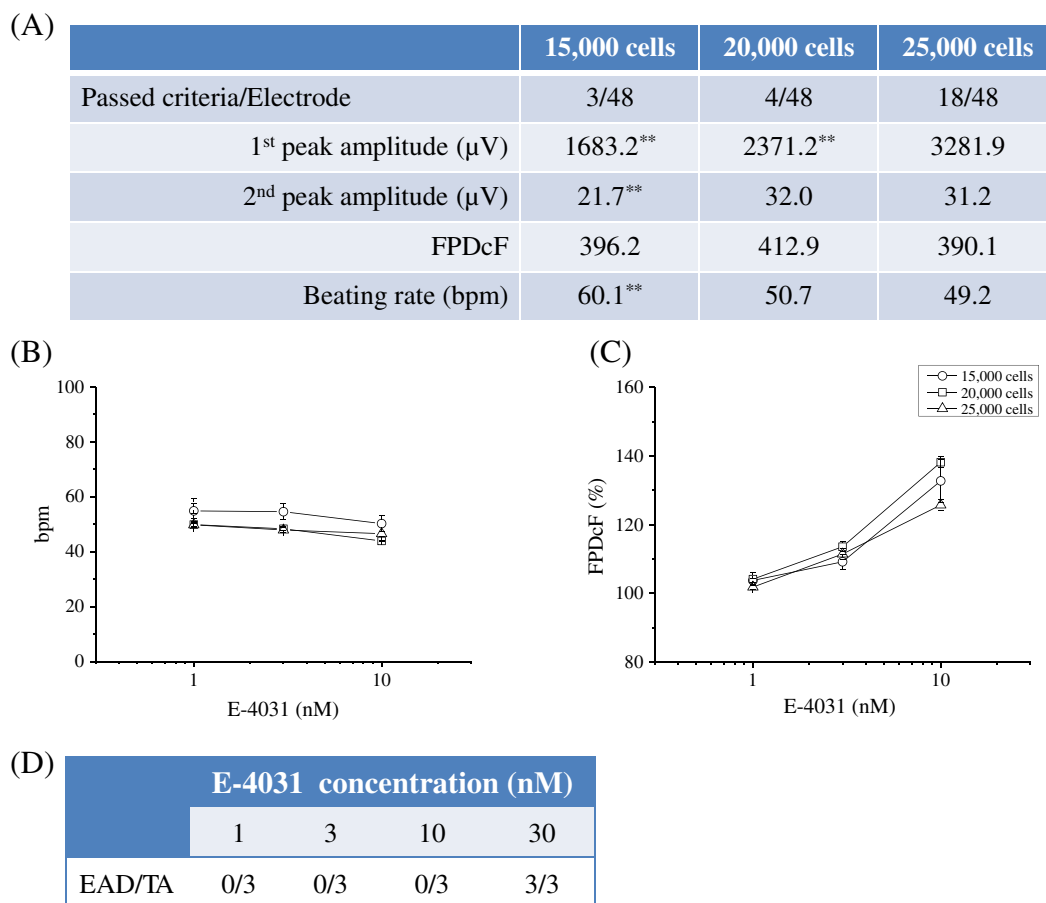
Table 1
Effects of test drugs on beat rate, corrected field potential duration with Fridericia's fomula (FPDcF), and first and second peak amplitude.

| Drug	Concentration		n	Beat rate (beats/min)		FPDcF (msec)		First peak amplitude (µV)		Second peak amplitude (µV)		EAD/TA
				HPF 0.1 Hz	HPF 1 Hz	HPF 0.1 Hz	HPF 1 Hz	HPF 0.1 Hz	HPF 1 Hz	HPF 0.1 Hz	HPF 1 Hz	
Aspirin	0	µM	7	60.4 ± 1.9	60.6 ± 1.7	409.8 ± 4.6	400.9 ± 4.3	2625 ± 591	2613 ± 582	33.7 ± 4.5	40.2 ± 4.4	
	3	µM	7	60.0 ± 1.8	60.0 ± 1.8	417.7 ± 2.4	408.1 ± 2.2	2672 ± 679	2670 ± 679	32.7 ± 4.9	38.4 ± 5.4	
	10	µM	7	60.0 ± 2.0	60.0 ± 2.0	417.4 ± 1.9	409.5 ± 2.0	2701 ± 739	2704 ± 738	33.0 ± 5.1	39.8 ± 5.9	
	30	µM	7	60.2 ± 2.3	60.2 ± 2.3	422.0 ± 3.0	413.8 ± 3.2	2782 ± 701	2785 ± 701	30.4 ± 6.5	37.6 ± 5.5	
	100	µM	7	60.7 ± 2.5	60.7 ± 2.5	421.9 ± 3.2	413.1 ± 3.6	2546 ± 736	2547 ± 735	32.2 ± 4.4	37.7 ± 5.3	
Terfenadine	0	µM	4	56.0 ± 0.8	56.0 ± 0.8	406.7 ± 7.0	399.5 ± 7.8	2764 ± 327	2765 ± 327	48.2 ± 9.6	59.0 ± 12.2	
	0.01	µM	4	53.1 ± 1.4	53.1 ± 1.4	436.8 ± 11.3	426.9 ± 11.8	3150 ± 420	3139 ± 415	60.8 ± 12.3	62.7 ± 13.2	
	0.03	µM	4	52.2 ± 1.6	51.8 ± 1.6	467.3 ± 16.3	454.1 ± 15.1	2831 ± 392	2849 ± 381	71.7 ± 11.2	64.2 ± 13.0	
	0.1	µM	4	51.6 ± 1.8	51.6 ± 1.8	499.2 ± 20.8	456.4 ± 17.3	2078 ± 455	2077 ± 454	60.7 ± 9.1	55.7 ± 13.5	
	0.3	µM	4	52.9 ± 0.9	52.9 ± 0.9	489.4 ± 5.3	415.1 ± 9.0	1114 ± 249	1155 ± 234	45.8 ± 9.2	55.5 ± 10.6	
Moxifloxacin	0	µM	6	52.5 ± 1.2	52.5 ± 1.2	452.4 ± 13.3	442.8 ± 11.4	1979 ± 453	1977 ± 453	43.6 ± 12.2	48.0 ± 7.4	
	10	µM	6	52.7 ± 1.9	52.7 ± 1.9	478.6 ± 12.6	468.6 ± 11.6	1800 ± 375	1796 ± 376	41.0 ± 11.3	44.4 ± 7.3	
	30	µM	5	55.0 ± 2.6	55.0 ± 2.6	523.3 ± 23.0	503.5 ± 19.0	1165 ± 189	1162 ± 190	36.9 ± 12.0	45.7 ± 7.9	EAD (1/6 samples)
	100	µM	4	47.4 ± 3.5	47.4 ± 3.5	628.9 ± 31.4	587.9 ± 24.9	1326 ± 635	1327 ± 635	34.4 ± 10.2	34.5 ± 6.7	EADs (2/6 samples)
	300	µM	0	n.c.	n.c.	n.c.	n.c.	n.c.	n.c.	n.c.	n.c.	EADs (6/6 samples)
Dimethyl sulfoxide	0	%	4	48.1 ± 1.3	48.0 ± 1.3	448.1 ± 8.2	439.8 ± 6.1	1768 ± 240	1745 ± 227	25.6 ± 7.5	28.1 ± 7.2	
	0.1	%	4	49.8 ± 1.2	49.8 ± 1.2	450.8 ± 9.3	442.8 ± 8.1	2261 ± 464	2262 ± 464	26.1 ± 7.3	27.3 ± 7.8	
	0.2	%	4	49.3 ± 1.5	49.3 ± 1.5	460.1 ± 8.4	453.4 ± 6.4	1815 ± 314	1813 ± 314	26.5 ± 7.7	26.7 ± 8.1	
	0.3	%	4	49.7 ± 1.6	49.7 ± 1.6	463.2 ± 8.5	456.1 ± 6.5	1965 ± 425	1964 ± 426	25.1 ± 6.7	26.2 ± 8.4	
	0.4	%	4	50.3 ± 1.4	50.3 ± 1.4	467.5 ± 9.2	459.5 ± 7.5	1799 ± 512	1799 ± 512	24.5 ± 6.4	25.2 ± 8.4	
	0.5	%	4	50.3 ± 1.9	50.3 ± 1.9	467.1 ± 12.5	462.5 ± 10.2	2008 ± 658	2008 ± 659	23.3 ± 6.3	24.1 ± 8.6	

Data are presented as mean ± SEM.
Control data (0 concentration) for aspirin, terfenadine, and moxifloxacin recorded by using vehicle (0.1% dimethyl sulfoxide).
EAD, early afterdepolarization; HPF, high-pass filter; n.c., not calculated; and TA, triggered activity.

(A)

	15,000 cells	20,000 cells	25,000 cells
Passed criteria/Electrode	3/48	4/48	18/48
1st peak amplitude (µV)	1683.2**	2371.2**	3281.9
2nd peak amplitude (µV)	21.7**	32.0	31.2
FPDcF	396.2	412.9	390.1
Beating rate (bpm)	60.1**	50.7	49.2

(B)

(C)

(D)

E-4031 concentration (nM)			
1	3	10	30
EAD/TA	0/3	0/3	0/3	3/3

Fig. 4. Effect of cardiomyocyte plating density on field potential (FP) parameters and response to E-4031. Cells were plated onto MED64 multi-electrode array probes at 15,000, 20,000, or 25,000 cells/2 µL/well (n = 3) and FP waveforms were recorded 7 days after plating. The average of each parameter was obtained by using 30 consecutive waveforms recorded after reaching a stable experimental condition. (A) Number of electrodes fulfilling the criteria first peak amplitude ≥ ±200 µV and second peak amplitude ≥15 µV, and the amplitude of the first and second peak calculated by using data obtained from 48 electrodes that recorded waveforms similar to that shown in Fig. 2C electrode No. 4. (B) The effects of E-4031 on FP duration corrected with Fridericia's formula (FPDcF) between different plating densities of cells (15,000, 20,000, or 25,000 cells/2 µL/well) were examined by cumulative application of E-4031 for 10 min at each concentration. The last 30 FP waveforms recorded were used for the analysis of beats per minute and FPDcF. (C) Incidence of early afterdepolarization or triggered activity (EAD/TA) during 10 min application of E-4031. **Paired t-test, P < 0.01 vs. 25,000 cells/2 µL/well.

(A)

(B)
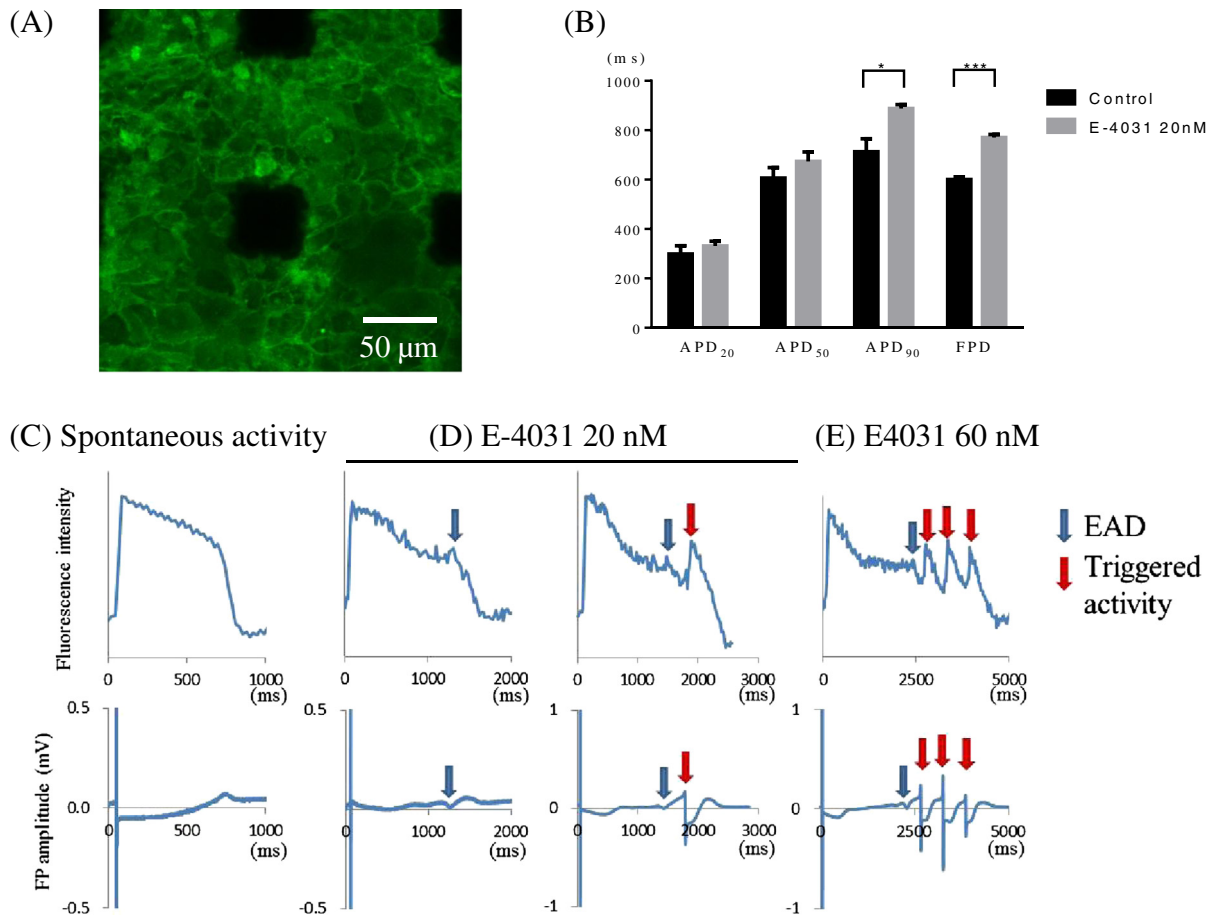
Fig. 5. Simultaneous measurement of field potential (FP) and action potential (AP) by using a voltage-sensitive dye (FluoVolt). Cells were plated at a density of 30,000 cells/2 μL onto MED64 multi-electrode array probes and cultured for 16 or 17 days. (A) Cells were treated with FluoVolt for 15 min and imaged under a fluorescence microscope with a 30× silicon oil immersion objective. FP waveforms were recorded through a 0.1-Hz high-pass filter on a MED64 multi-electrode array system, and AP waveforms were recorded as a FluoVolt fluorescence signal. (B) Effects of the addition of 20 nM of E-4031 to the culture medium on AP duration (APD) at 20%, 50%, and 90% repolarization (APD$_{20}$, APD$_{50}$, APD$_{90}$), and FP duration (FPD), prior to the occurrence of early afterdepolarization (EAD) (n = 3). FPD and APD were measured in three corresponding FP and AP waveforms. Values are presented as mean ± SEM. *$P < 0.05$, ***$P < 0.001$ compared with the control values. Typical corresponding waveforms under conditions of (C) spontaneous activity, (D) E-4031 at 20 nM (left, initial phase of EAD induction; right, 6 min after EAD induction), and (E) E-4031 at 60 nM on AP and FP.

high (i.e., 1 Hz), because the second peak contained the slow components of the current (Figs. 2 and 3). Thus, the FP waveform recorded through the 1-Hz HPF was strongly affected by the differentiator circuit in the MEA amplifier compared with that recorded through the 0.1-Hz HPF, leading to peak attenuation and a phase shift in the waveform (Fig. 3E). In addition, negative waveforms after second peak were often observed when a 1-Hz HPF was used. However, since these negative waveforms after second peak were not observed when a 0.1-Hz HPF was used, it is likely that they were artifacts created by the resistor–capacitor circuit differentiation.

As shown in Fig. 2C (electrode No. 4), when the amplitude of the second peak was sufficiently large and sharp, similar waveforms were obtained whether a 0.1- or 1-Hz HPF was used. However, when the amplitude of the second peak was small (e.g., electrode No. 5) the waveforms were strikingly different between the two frequencies of HPF; indeed, in the waveform detected by electrode No. 5, when a 1-Hz HPF was used the second peak was observed, but when a 0.1-Hz HPF was used the second peak was not observed, which may be due to the differentiator circuit in the MEA amplifier. Concerns related to the differentiation associated with HPFs become an issue when attempting to evaluate the effects of a drug. When terfenadine was added to the culture medium (Fig. 3C), there was a marked difference in the concentration–response curves recorded through the 0.1- and 1-Hz HPFs. This may be a result of a phase shift when the 1-Hz HPF was used (Fig. 3E). For the negative plateau potential between the first and second peaks, it is likely that the FP waveforms recorded through a 0.1-Hz HPF reflect

inward currents such as I$_{Ca}$ (calcium current) and I$_{NCX}$ (sodium–calcium exchange current) unlike those recorded through a 1-Hz HPF. Since FP waveforms can be considered a composite representation of the membrane potential and several ionic currents, a future challenge will be the evaluation of the effects of a multi-channel blocker such as terfenadine on the shapes of the FP waveform. Furthermore, since this was the first time that these waveform changes have been successfully recorded through a 0.1-Hz HPF, a quantitative analytical method to assess these changes is now needed. Thus, since a high HPF frequency may lead to misinterpretation of drug effect, and a lower HPF frequency can be used to clearly record various changes in the waveform between the first and second peaks, especially slow component changes, HPF frequency is clearly an important factor to take into consideration when accurately evaluating drug effects using an MEA system. Therefore, we recommend that a 0.1-Hz HPF be used when recording FP waveforms of human iPS-derived cardiomyocytes.

4.3. Effect of acquisition conditions on FP waveform

Although the plating of cells at low density (<3750 cells/probe) has been reported to alter both the response to hERG inhibitors and the I$_{Ks}$ current due to the reduction in the expression of I$_{Ks}$ and I$_{K1}$ channels, higher densities (7500–30,000 cells/probe) have been shown to not alter cellular sensitivity to these inhibitors (Uesugi, Ojima, Taniguchi, Miyamoto, & Sawada, 2014). The present results were consistent with these previous findings in that there were no changes in the

concentration–response curves for E-4031 when cells were plated at densities of 15,000, 20,000, or 25,000 cells/well. However, the amplitude of the first and second peaks did tend to increase as cell density increased. One possible explanation for this is that cell density affects the relationship between the cardiomyocyte cell membrane and the electrode surface. At higher cell densities, the distance between the cell membrane and the electrode surface is likely to be closer and therefore cleft resistance higher, which would result in a higher voltage signal and more accurate FP waveforms. Furthermore, plating cells at high density may cause layering of the cells on the electrodes, producing tighter cell-to-electrode and cell-to-cell seals in proportion to cell plating density. Other factors such as cell-adhesion molecules activity, electrode surface composition, and coating reagent type (e.g., fibronectin) may also affect the relationship between cardiomyocytes and the electrode surface.

In the present study, the experimental conditions, including experimenters, cell type, cell lot, fibronectin maker, fibronectin lot, and experiment day were the kept the same. Seeding cells at a density of 15,000, 20,000, or 25,000 cells/well did not affect drug responses when the FP waveform on the MEA electrodes was selected for analysis according to our criteria. Our observations, together with the influence of the seeding cell densities reported previously (Nakamura et al., 2014; Uesugi et al., 2014), suggest that higher densities of cardiomyocytes and identical experimental conditions, especially for validation studies in which multiple facilities participate, should be used in MEA-based experiments.

4.4. Relationship between FP and AP

Since FP signals are derived from the relationship between the cardiomyocyte cell membrane and the electrode surface, and are not a direct measure of membrane current or AP, FP waveforms can be difficult to interpret. Although a liner relationship between APD and FPD has been implicated in mouse cardiomyocytes (Halbach, Egert, Hescheler, & Banach, 2003), to further understand the relationship between FP and AP, we simultaneously recorded AP and FP waveforms (Fig. 5C). The first peak of the FP waveform closely corresponded to the initial upstroke of the AP waveform, indicating the likely contribution of Na^+ channels to the first peak in the FP waveform. The second peak of the FP waveform occurred roughly at the beginning of the later repolarization phase of the AP waveform, and FPD corresponded to APD_{50} under basal conditions (Fig. 5B), suggesting the contribution of I_{Kr} or I_{Ks} (slow component of delayed rectifier K^+ current), or both, to the current. The plateau phase of the AP waveform corresponded to the negative phase between the first and second peaks of the FP waveform, suggesting that the amplitude of the negative plateau potential was associated with the influx of calcium ions. Furthermore, the occurrence of EAD and TA in the FP waveform, which was induced by E-4031, was also reflected in the AP waveform (Fig. 5C). Together these results suggest that the analysis of the effects of drug candidates on ionic currents and proarrhythmic potential would be greatly enhanced by using a combination of FP and AP data.

4.5. Limitations of FPD evaluation and future steps

Although the recording of FP with an MEA-based system is a useful method, our results suggest that changes in the FP waveform do not accurately reflect the drug effect when the second peak in the FP waveform is greatly reduced by the presence of a drug. The effect of the HPF is a further concern in the analysis of FP. Thus, despite the potential advantages of evaluating FPD by using an MEA-based system for the electrophysiological characterization of the effect of drugs on iPS cell-derived cardiomyocytes, careful attention should be paid to the data analysis with regard to alteration of the FP waveform. These problems are expected to be addressed as improvements are made to MEA systems (Spira & Hai, 2013), and the combination of other evaluation methods and systems such as motion vector prediction (Hayakawa et al., 2014),

calcium imaging, and electrical impedance together with the MEA system (Peters, Lamore, Guo, Scott, & Kolaja, 2015) are expected to produce more accurate drug evaluations.

Appendix 1. Electrical circuit of the cardiomyocyte sheet–electrode interface

The extracellular FP originates from changes in ion concentration in the cleft between cells that are a result of the activation of ion channels in the plasma membrane. When cleft resistance (R_{seal} in Fig. 1A) is high, for example when there is tight association between a cardiomyocyte cell membrane and an electrode, the difference in ionic concentration between the cleft and bulk solution will give rise to a potential difference that can be detected by the electrode. Therefore, ideally, the FP signal represents the total membrane current producing the change in ionic concentration in the cleft (e.g., the FP waveform shown in Fig. 2C, electrode No. 4). Signal amplitude is greater when the volume of the cleft is smaller, due to better seal formation between the cell membrane and electrodes. When the resistance in the cleft (R_{seal}) is extremely high or when the resistance in the cell membrane (R_j) is decreased, the voltage in the cleft will be affected by the intracellular voltage and may possibly represent the intracellular voltage. An example of this is the phenomenon where the production of an AP-like waveform is induced by application of strong biphasic electrical pulses to the bipolar electrodes that make the plasma membrane slightly leaky, as shown in Fig. 1C, which decreases the plasma membrane resistance (Spira & Hai, 2013).

In the present study, there was a large degree of variation in the waveforms recorded by the individual electrodes in the array, suggesting that the optimal configuration of the cell membrane and electrodes was not always established, or that mixed FP and AP signals were recorded by many of the electrodes (Fig. 2A). Movement by the contraction of the cardiomyocytes may also affect the shape of the waveform recorded by altering the spatial relationship between cell membrane and electrode.

Appendix 2. Effect of HPF frequency on FP waveform

In the present study, MEA electrodes were used to detect changes in extracellular potential, which reflect the depolarization and hyperpolarizing of the cardiomyocyte cell membrane. Currents flowing into cells were detected as negative voltages and currents flowing out of cells were detected as positive currents. A major portion of these currents are a result of Na^+, K^+, and Ca^{2+} ions flowing through ion channels in the cell membrane and their compensating capacitive currents. The ionic currents in the cardiomyocyte cell membrane vary from the very fast I_{Na} current to the slow I_{Kr} and I_{Ks} currents. Therefore, the frequency of the HPF is important for acquiring accurate FP waveform data. Fast currents such as I_{Na} underlying the first peak in the FP

waveform, which peaks within 1 msec from the voltage clamp experiment of the I_{Na} current in iPS-derived cardiac cells (Ma et al., 2011) will be influenced by a low-pass filter set below 1000 Hz. In contrast, the slow currents such as I_{Kr} and I_{Ks} underlying the second peak will be influenced more by a HPF (Figs. 2 and 3). In the measurement of bioelectrical signals, HPFs are generally used to eliminate the very-low-frequency component that causes the electrical signal to drift. HPFs are generally implemented as a resistance–capacitor circuit, in which, the current (I) that flows through a capacitor (C) with resistance (R), input voltage (V_i), and output voltage (V_o), can be expressed as follows:

$$I = C \times \frac{d(V_i - V_o)}{dt}.$$

From Ohm's law ($V = I \cdot R$), therefore

$$V_o = R \cdot C \times \frac{d(V_i - V_o)}{dt},$$

and

$$\left(1 + R \cdot C \times \frac{d}{dt}\right) V_o = R \cdot C \times \frac{dV_i}{dt}.$$

Since voltage becomes approximately constant over time (t) when the change of voltage signals are far lower than the lower cutoff frequency,

$$\frac{dV_o}{dt} = 0.$$

Therefore,

$$V_o = R \cdot C \times \frac{dV_i}{dt}.$$

Thus, V_o will be differentiated compared with V_i through the resistance–capacitor circuit.

In addition, the output voltage when a sine wave is input to a differentiation circuit can be expressed as

$$V_o = \frac{d(V_i)}{dt} = \frac{d(\sin(2\pi \cdot f \cdot t))}{dt} = 2\pi \cdot f \cdot \cos(2\pi \cdot f \cdot t).$$

References

Cavero, I. (2014). 13th Annual Meeting of the Safety Pharmacology Society: Focus on novel technologies and safety pharmacology frontiers. *Expert Opinion on Drug Safety, 13*(9), 1271–1281.

Cavero, I., & Holzgrefe, H. (2014). Comprehensive *in vitro* Proarrhythmia Assay, a novel *in vitro/in silico* paradigm to detect ventricular proarrhythmic liability: A visionary 21st century initiative. *Expert Opinion on Drug Safety, 13*(6), 745–758.

Fejtl, M., Stett, A., Nisch, W., Boven, K.H., & Möller, A. (2006). On micro-electrode array revival: Its development, sophistication of recording, and stimulation. *Advances in network electrophysiology* (pp. 24–37). US: Springer.

Gibson, J.K., Yue, Y., Bronson, J., Palmer, C., & Numann, R. (2014). Human stem cell-derived cardiomyocytes detect drug-mediated changes in action potentials and ion currents. *Journal of Pharmacological and Toxicological Methods, 70*(3), 255–267.

Gintant, G. (2011). An evaluation of hERG current assay performance: translating preclinical safety studies to clinical QT prolongation. *Pharmacology & Therapeutics, 129*(2), 109–119.

Halbach, M.D., Egert, U., Hescheler, J., & Banach, K. (2003). Estimation of action potential changes from field potential recordings in multicellular mouse cardiac myocyte cultures. *Cellular Physiology and Biochemistry, 13*(5), 271–284.

Harris, K., Aylott, M., Cui, Y., Louttit, J.B., McMahon, N.C., & Sridhar, A. (2013). Comparison of electrophysiological data from human-induced pluripotent stem cell–derived cardiomyocytes to functional preclinical safety assays. *Toxicological Sciences, 134*(2), 412–426.

Hayakawa, T., Kunihiro, T., Ando, T., Kobayashi, S., Matsui, E., Yada, H., et al. (2014). Image-based evaluation of contraction–relaxation kinetics of human-induced pluripotent stem cell-derived cardiomyocytes: Correlation and complementarity with extracellular electrophysiology. *Journal of Molecular and Cellular Cardiology, 77*, 178–191.

Hayashi, S., Kii, Y., Tabo, M., Fukuda, H., Itoh, T., Shimosato, T., et al. (2005). QT PRODACT: A multi-site study of in vitro action potential assays on 21 compounds in isolated guinea-pig papillary muscles. *Journal of Pharmacological Sciences, 99*(5), 423–437.

Kaneko, T., Nomura, F., Hamada, T., Abe, Y., Takamori, H., Sakakura, T., et al. (2014). On-chip in vitro cell-network pre-clinical cardiac toxicity using spatiotemporal human cardiomyocyte measurement on a chip. *Scientific Reports, 4*(Article number: 4670).

Lu, H.R., Vlaminckx, E., Hermans, A.N., Rohrbacher, J., Van Ammel, K., Towart, R., et al. (2008). Predicting drug-induced changes in QT interval and arrhythmias: QT-shortening drugs point to gaps in the ICHS7B Guidelines. *British Journal of Pharmacology, 154*(7), 1427–1438.

Ma, J., Guo, L., Fiene, S.J., Anson, B.D., Thomson, J.A., Kamp, T.J., et al. (2011). High purity human-induced pluripotent stem cell-derived cardiomyocytes: Electrophysiological properties of action potentials and ionic currents. *American Journal of Physiology. Heart and Circulatory Physiology, 301*(5), H2006–H2017.

Martin, R.L., McDermott, J.S., Salmen, H.J., Palmatier, J., Cox, B.F., & Gintant, G.A. (2004). The utility of hERG and repolarization assays in evaluating delayed cardiac repolarization: Influence of multi-channel block. *Journal of Cardiovascular Pharmacology, 43*(3), 369–379.

Meiry, G., Reisner, Y., Feld, Y., Goldberg, S., Rosen, M., Ziv, N., et al. (2001). Evolution of action potential propagation and repolarization in cultured neonatal rat ventricular myocytes. *Journal of Cardiovascular Electrophysiology, 12*(11), 1269–1277.

Meyer, T., Boven, K.H., Günther, E., & Fejtl, M. (2004). Micro-electrode arrays in cardiac safety pharmacology. *Drug Safety, 27*(11), 763–772.

Nakamura, Y., Matsuo, J., Miyamoto, N., Ojima, A., Ando, K., Kanda, Y., et al. (2014). Assessment of testing methods for drug-induced repolarization delay and arrhythmias in an iPS cell-derived cardiomyocyte sheet: Multi-site validation study. *Journal of Pharmacological Sciences, 124*(4), 494–501.

Nozaki, Y., Honda, Y., Tsujimoto, S., Watanabe, H., Kunimatsu, T., & Funabashi, H. (2014). Availability of human induced pluripotent stem cell-derived cardiomyocytes in assessment of drug potential for QT prolongation. *Toxicology and Applied Pharmacology, 278*(1), 72–77.

Obiol-Pardo, C., Gomis-Tena, J., Sanz, F., Saiz, J., & Pastor, M.A. (2011). A multiscale simulation system for the prediction of drug-induced cardiotoxicity. *Journal of Chemical Information and Modeling, 51*, 483–492.

Peng, S., Lacerda, A.E., Kirsch, G.E., Brown, A.M., & Bruening-Wright, A. (2010). The action potential and comparative pharmacology of stem cell-derived human cardiomyocytes. *Journal of Pharmacological and Toxicological Methods, 61*(3), 277–286.

Peters, M.F., Lamore, S.D., Guo, L., Scott, C.W., & Kolaja, K.L. (2015). Human stem cell-derived cardiomyocytes in cellular impedance assays: Bringing cardiotoxicity screening to the front line. *Cardiovascular Toxicology, 15*(2), 127–139.

Pine, J. (2006). A history of MEA development. In M. Taketani, & M. Baudru (Eds.), *Advances in network electrophysiology.* (pp. 3–23)US: Springer.

Redfern, W.S., Carlsson, L., Davis, A.S., Lynch, W.G., MacKenzie, I., Palethorpe, S., et al. (2003). Relationships between preclinical cardiac electrophysiology, clinical QT interval prolongation and torsade de pointes for a broad range of drugs: Evidence for a provisional safety margin in drug development. *Cardiovascular Research, 58*(1), 32–45.

Sager, P.T., Gintant, G., Turner, J.R., Pettit, S., & Stockbridge, N. (2014). Rechanneling the cardiac proarrhythmia safety paradigm: A meeting report from the Cardiac Safety Research Consortium. *American Heart Journal, 167*(3), 292–300.

Spira, M.E., & Hai, A. (2013). Multi-electrode array technologies for neuroscience and cardiology. *Nature Nanotechnology, 8*(2), 83–94.

Tanaka, T., Tohyama, S., Murata, M., Nomura, F., Kaneko, T., Chen, H., et al. (2009). In vitro pharmacologic testing using human induced pluripotent stem cell-derived cardiomyocytes. *Biochemical and Biophysical Research Communications, 385*(4), 497–502.

Thomas, C.A., Jr., Springer, P.A., Loeb, G.E., Berwald-Netter, Y., & Okun, L.M. (1972). A miniature microelectrode array to monitor the bioelectric activity of cultured cells. *Experimental Cell Research, 74*(1), 61–66.

Uesugi, M., Ojima, A., Taniguchi, T., Miyamoto, N., & Sawada, K. (2014). Low-density plating is sufficient to induce cardiac hypertrophy and electrical remodeling in highly purified human iPS cell-derived cardiomyocytes. *Journal of Pharmacological and Toxicological Methods, 69*(2), 177–188.

Egert, Ulrich, & Meyer, Thomas (2005). Heart on a Chip – Extracellular Multielectrode Recordings from Cardiac Myocytes in Vitro. *Practical Methods in Cardiovascular Research, pp*, 432–453.

Egert, Ulrich, Banach, Kathrin, & Meyer, Thomas (2006). Analysis of Cardiac Myocyte Activity Dynamics with Micro-Electrode Arrays. *Advances in Network Electrophysiology, pp*, 274–290.

Yamazaki, K., Hihara, T., Kato, H., Fukushima, T., Fukushima, K., Taniguchi, T., et al. (2014). Beat-to-beat variability in field potential duration in human embryonic stem cell-derived cardiomyocyte clusters for assessment of arrhythmogenic risk, and a case study of its application. *Pharmacology and Pharmacy, 5*, 117–128.

Yamazaki, K., Hihara, T., Taniguchi, T., Kohmura, N., Yoshinaga, T., Ito, M., et al. (2012). A novel method of selecting human embryonic stem cell-derived cardiomyocyte clusters for assessment of potential to influence QT interval. *Toxicology in Vitro, 26*(2), 335–342.